# (*Z*/*E*)-Photoisomerization of $C_{40}$-Carotenoids by Iodine

**Péter Molnár and József Szabolcs** *,†
*Institute of Chemistry, Pécs University Medical School, 7643 Pécs, Hungary*

---

The compositions of stereoisomeric mixtures of β-carotene (**1**), zeaxanthin (**2**), physaliene (**3**), natural violaxanthin (**4**), 'semi-synthetic' violaxanthin (**5**), capsorubin (**6**), capsanthin (**7**) and lutein-epoxide (**8**) have been investigated. The effect of end groups with different structures and stereochemistry on the *cis–trans* equilibrium, the rates of photo-induced *cis–trans* rearrangement of the zeaxanthin (**2**) set, and the 'specific rate' (per unit light energy at a given wavelength) for several 13-*cis* carotenoids (**2**, **4**, **6**, **7**, **9**) have been determined.

---

(*Z*/*E*)-Photoisomerization by iodine catalysis was introduced into the chemistry of carotenoids by P. Karrer *et al.*[1] who showed that, on exposure to iodine, natural bixin (*cis* form) converted into β-bixin (*trans* form). The subsequent extensive studies by Zechmeister and his co-workers[2–5] revealed the main factors that influence iodine-catalysed photo-stereomutation of $C_{40}$-carotenoids. In spite of the detailed work already done on geometrical isomerism of carotenoids,[6–19] few studies have dealt with the kinetics and mechanism of this process.[7,20–23]

The whole phenomenon of iodine-catalysed *cis–trans* photoisomerization of carotenoids is illustrated in a summary diagram (Fig. 1). The progress of *cis–trans* stereomutation of 13-*cis*-zeaxanthin (13-*cis*-**2**), in response to different irradiations, is plotted *vs.* time: the horizontal line AB indicates that, in the absence of iodine and in the dark, there is no *cis–trans* isomerization. The curve from A to H shows, in the presence of iodine, the variation with different conditions. Even without light (AC), *cis–trans* isomerization proceeds rather slowly. At first, the curve segment CF shows a moderately steep (CD) and a steep (DE) upward trend; then it passes through a maximum (F), which corresponds to the state of quasi-equilibrium with the maximum content of the all-*trans* form. The smooth decrease (FG) is due to the formation of di-*cis* and poly-*cis* isomers and some irreversible reactions. The curve from G to H falls to zero as the geometrical isomers decompose to colourless substances ('bleaching') *via* irreversible reactions which become dominant.

In this paper we reinvestigate the phenomenon by using authentic *cis*-carotenoids and improved analytical methods.

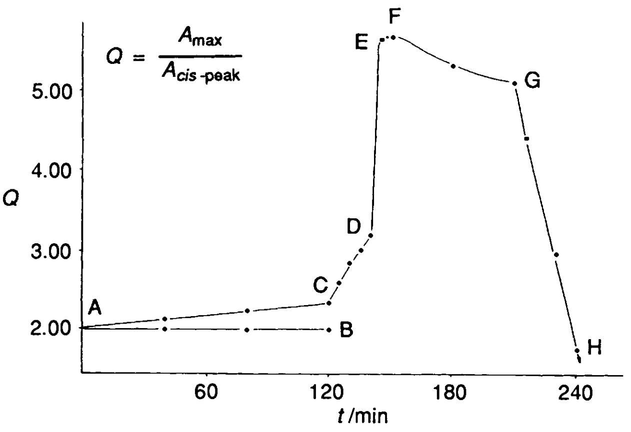

**Fig. 1** Isomerization of 13(15)-*cis*-zeaxanthin [13(15)-*cis*-**2**] ($10^{-5}$ mol $dm^{-3}$ in benzene, 24 °C) in the absence of iodine in darkness (AB): by iodine catalysis (2% $I_2$) in darkness (AC), in red light ($\lambda$ > 625 nm: CD), in diffuse daylight (DG) and in sunlight (GH)

## Results and Discussion

*Composition of Stereoisomeric Mixtures.*—To study the composition of equilibrium mixtures, and the influence of the structure and stereochemistry of end groups on the composition, we started from Zechmeister's classic results,[2–5] using the best known $C_{40}$-carotenoids (**1**, **2**, **3**, **4**, **5**, **6**, **7**, **8**). These experiments (Table 1) revealed the following.

(*a*) A quasi-equilibrium was reached within 20–60 min.

(*b*) The composition of quasi-equilibrium mixtures was independent of the direction of the stereomutation, *i.e.* it made only a slight difference whether the stereomutation had begun from the all-*trans* or the *cis*-forms.

(*c*) After a longer period of time the quasi-equilibrium was disturbed by the formation of poly-*cis* isomers (Scheme 1) and various irreversible side-reactions (bleaching,[5,10] 5,6-epoxide–5,8-epoxide rearrangement,[6,7,10] *etc.*).

(*d*) The all-*trans* form was predominant.

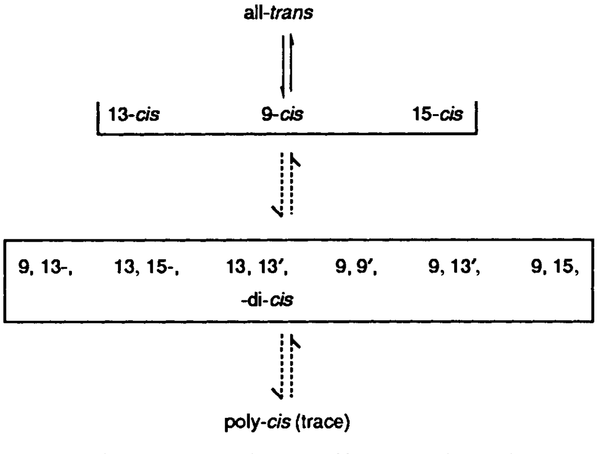

**Scheme 1** The complex equilibrium of iodine-catalysed photoisomerization of symmetrical $C_{40}$-carotenoids

(*e*) The equilibrium mixtures were very similar in composition for each carotenoid.

(*f*) Carotenoids having symmetrical structures (**2**, **3**, **4**, **5**, **6**) yielded 9-, 13- and 15-mono-*cis* isomers,[7,10,11,13,15] while those with unsymmetrical structures (**7**, **8**) gave 9-, 9′-, 13-, 13′- and 15-mono-*cis* isomers.[7,10,14,18]

(*g*) The 15(= central)-mono-*cis* isomers[13,15,18] were always present in the equilibrium mixtures.

(*h*) The different cyclic end groups (β-, 3-hydroxy-β-, 3-hexadecoxycarbonyl-β-, 3-hydroxy-5,6-epoxy-β- and ε-end group) which attached themselves to the same chromophoric

---

† *Present address:* H-9300 Csorna, Szent István tér 17, Hungary.

**Table 1** Composition of equilibrium mixtures of several symmetrical and asymmetrical $C_{40}$-carotenoids isomerized by iodine in diffuse daylight for 20–60 min at 25 °C (in benzene)

| | $Q = A_{max}/A_{cis\text{-}peak}$ | | Percentage of isomers in the equilibrium | | | | |
|---|---|---|---|---|---|---|---|
| Starting material | Starting material | Equilibrium mixture | all-*trans* | 9-*cis* | 13-cis | 15-*cis* | di-*cis* |
| β,β-Carotene (**1**) | >10 | 4.35 | 49.1 | 24.8 | 18.9 | | 7.1 |
| Zeaxanthin (**2**) | >10 | 5.07 | 54.4 | 23.5 | 10.8 | 2.0 | 9.4 |
| 9-*cis*-**2** | 6.43 | 5.05 | 53.7 | 24.2 | 11.2 | 2.1 | 8.8 |
| 13(15)-*cis*-**2** | 2.07 | 5.05 | 55.2 | 22.2 | 12.3 | 2.4 | 8.1 |
| Average value | — | 5.05 ± 0.01 | 54.4 ± 0.6 | 23.2 ± 0.9 | 11.4 ± 0.8 | 2.2 ± 0.2 | 8.8 ± 0.5 |
| Physaliene (**3**) | >10 | 5.84 | 52.8 | 21.4 | 15.0 | | 10.8 |
| 3*S*,5*R*,6*S*,3′*S*,5′*R*,6′*S*-Violaxanthin (**4**) | >10 | 5.80 | 51.8 | 23.8 | 10.5 | 1.9 | 12.1 |
| 9-*cis*-**4** | 11.94 | 6.00 | 52.3 | 23.7 | 10.2 | 1.8 | 12.0 |
| 13-*cis*-**14** | 1.98 | 5.80 | 49.4 | 24.4 | 13.9 | 2.5 | 9.8 |
| 15-*cis*-**4** | 1.65 | 5.50 | 50.0 | 23.3 | 11.9 | 2.1 | 11.3 |
| Average value | — | 5.78 ± 0.18 | 50.9 ± 1.2 | 23.8 ± 0.5 | 11.6 ± 1.8 | 2.1 ± 0.3 | 11.3 ± 0.9 |
| 3*S*,5*S*,6*R*,3′*S*,5′*S*,6′*R*-Violaxanthin (**5**) | >10 | 8.05 | 53.7 | 22.2 | 13.0 | | 11.1 |
| 9-*cis*-**5** | 17.50 | 8.10 | 55.2 | 23.6 | 12.8 | | 8.5 |
| 13(15)-*cis*-**5** | 1.93 | 6.25 | 52.7 | 22.3 | 14.4 | | 10.5 |
| Average value | — | 7.47 ± 0.86 | 53.9 ± 1.0 | 22.7 ± 0.6 | 13.4±0.7 | | 10.0 ± 1.1 |
| Capsorubin (**6**) | >10 | 7.36 | 66.0 | 16.3 | 15.1 | | 2.6 |
| 9-*cis*-**6** | 10.03 | 7.40 | 65.4 | 16.6 | 15.6 | | 2.4 |
| 13(15)-*cis*-**6** | 2.26 | 7.42 | 65.3 | 16.9 | 15.0 | | 2.8 |
| Average value | — | 7.39 ± 0.03 | 65.6 ± 0.9 | 16.6 ± 0.3 | 15.2±0.2 | | 2.6 ± 0.2 |
| Capsanthin (**7**) | 9.50 | 4.37 | 56.9 | 18.9[a] | 14.6[b] | | 9.6 |
| 9(9′)-*cis*-**7** | 4.44 | 4.63 | 53.6 | 19.3 | 16.2 | | 10.9 |
| 13[13′(15)]-*cis*-**7** | 1.80 | 4.67 | 55.9 | 19.5 | 16.2 | | 8.4 |
| Average value | — | 4.56 ± 0.12 | 55.5 ± 1.2 | 19.2 ± 0.2 | 15.7±0.7 | | 9.6 ± 0.8 |
| Lutein epoxide (**8**) | >10 | 6.70 | 56.4 | 23.1[a] | 10.5[c] | 2.2 | 8.7 |
| 9(9′)-*cis*-**8** | 12.83 | 7.00 | 53.2 | 22.4 | 12.9 | 2.7 | 8.8 |
| 13[13′(15)]-*cis*-**8** | 1.98 | 6.85 | 56.6 | 22.2 | 12.4 | 2.5 | 6.3 |
| Average value | — | 6.85 ± 0.12 | 55.4 ± 1.6 | 22.6 ± 0.4 | 11.9 ± 1.0 | 2.5 ± 0.2 | 7.9 ± 1.2 |

[a] Mixture of 9- and 9′-*cis*-isomers. [b] Mixture of 13-, 13′- and 15-*cis*-isomers. [c] Mixture of 13- and 13′-*cis*-isomers.

nonaene chain (**1**, **2**, **3**, **4**, **5**, **8**) influenced the percentage composition of equilibrium mixtures only slightly (within experimental error).

(*i*) No significant difference in percentage composition was observed between the equilibrium mixtures of carotenoids with end groups of different stereochemistry (**4**, **5**).

(*j*) The ratio of mono-*cis* forms to di-*cis* forms *in toto* was *ca.* 3.6–4.2.

(*k*) If both cyclic end groups were separated from the terminal C-7 and C-7′ atoms of the polyene chain by carbonyl groups (capsorubin, **6**) in equilibrium mixtures, the amount of the all-*trans* form increased at the expense of the 9-mono-*cis* form.

Considering the different composition of the equilibrium mixture for **6**, at first it was believed that in the capsorubin molecule, the steric conflict between one of the C-16, C-17 and C-18 methyl groups and a hydrogen atom at C-8 had diminished, *i.e.* the thermodynamic stability of the all-*trans* form had increased. However, capsanthin (**7**), the end groups of which have a structure identical with that of **6** and **2**, contradicted this assumption since it gave a quasi-equilibrium mixture of the usual percentage composition. Probably, the cooperation of the effects of the two terminal carbonyl groups in the polyene chain of **6** could result in an increased stability for the *trans* form compared to that of **7**, *i.e.* in an increase in the percentage of all-*trans*-capsorubin (**6**) in the quasi-equilibrium mixture.

*Rate Experiments.*—The complex equilibrium of iodine catalysed photoisomerization of even symmetrical $C_{40}$-carotenoids (**1**, **2**, **4**) consists of too many parallel and consecutive first-order reactions with reversible reaction steps for kinetic calculations[24,25] to be applicable (Scheme 1). In addition, the amount of the individual di- and poly-*cis* isomers cannot be determined with accuracy. Therefore, we limited ourselves to graphical representation by plotting the changes in the mole fractions of isomers *vs.* time. As one of the simplest models, the zeaxanthin set (**2**) in benzene solution was used in diffuse laboratory daylight. The loss of pigments was negligible: recovery was 98%. Comparison of the curves and the regression coefficients for the slopes of the straight line segments in Figs. 2, 3 and 4 led to the following conclusions.

(*a*) The rate of conversion of a geometrical isomer depends on the geometrical configuration: rate (9-*cis*) > rate [13(15)-*cis*]* ~ rate (*trans*).

(*b*) The rate of formation of a geometrical isomer depends on the geometrical configuration of the starting isomer: rate (*trans* from 9-*cis*) > rate [*trans* from 13(15)-*cis*], rate (9-*cis* from *trans*) > rate [9-*cis* from 13(15)-*cis*], rate [13(15)-*cis* from *trans*] ~ rate [13(15)-*cis* from 9-*cis*], rate (total di-*cis* from 9-*cis*) > rate [total di-*cis* from 13(15)-*cis*] > rate (total di-*cis* from *trans*).

---

* 13(15)-*cis* = 13-*cis* + 15-*cis* (mixture of 13- and 15-*cis*-isomers).

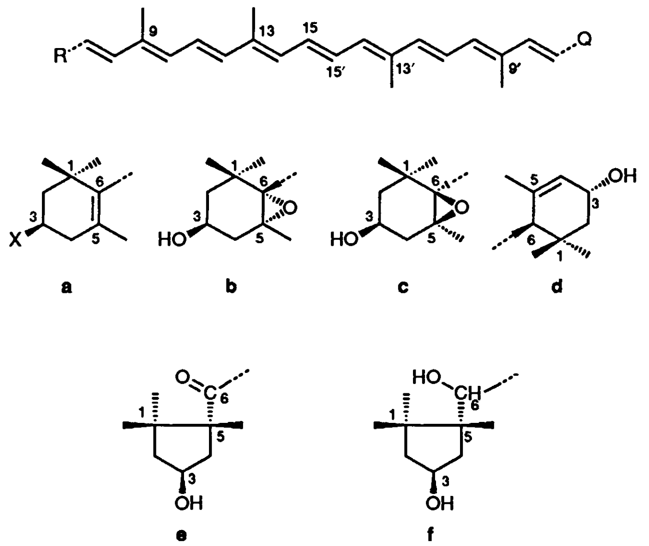

1: β,β-Carotene (R = Q = a; X = H)
2: Zeaxanthin (R = Q = a; X = OH)
3: Physaliene (R = Q = a; X = $OCOC_{15}H_{31}$)
4: 3*S*,5*R*,6*S*,3′*S*,5′*R*,6′*S*-Violaxanthin (R = Q = b)
5: 3*S*,5*S*,6*R*,3′*S*,5′*S*,6′*R*-Violaxanthin (R = Q = c)
6: Capsorubin (R = Q = e)
7: Capsanthin (R = a, X = OH; Q = e)
8: 3*S*,5*R*,6*S*,3′*R*,6′*R*-Lutein-epoxide (R = b; Q = d)
9: Capsanthol (R = a, X = OH; Q = f)

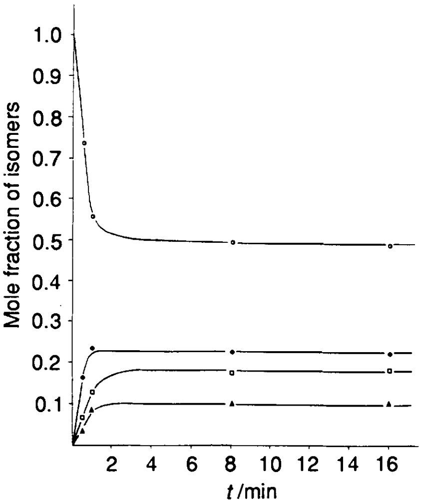

**Fig. 2** Isomerization of all-*trans*-zeaxanthin (**2**) ($10^{-4}$ mol dm$^{-1}$ in benzene, 24 °C) by iodine catalysis (2% $I_2$) in diffuse daylight (○——○ all-*trans*, ●——● 9-*cis*, □——□ 13(15)-*cis*, ▲——▲ mixture of di-*cis*-isomers)

It can be seen that, with the exception of 13(15)-*cis*-zeaxanthin [13(15)-*cis*-**2**], the rate of formation of a mono-*cis* isomer was greater from the all-*trans* form than from the other mono-*cis* forms.

For a prolonged time ($t > 40$ min), the formation of geometrical isomers exhibited a curved response downward towards the time axis. This behaviour was certainly due to irreversible loss of pigments.[5,10]

Computations[26] of the experimental data (Table 2) gave either linear ($Y = at + b$) or exponential [$Y_1{}^* = A{\cdot}e^{at+b} + B$, $Y_2{}^* = A(1 - e^{at+b})$] functions, allowing no generalization. The linear functions were calculated by using two sets of parameters for two different time intervals. The number of experimental data points was not sufficient for more accurate computations.

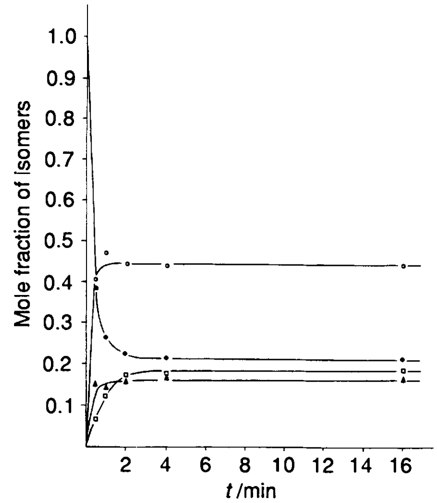

**Fig. 3** Isomerization of 9-*cis*-zeaxanthin (9-*cis*-**2**) ($10^{-4}$ mol dm$^{-3}$ in benzene, 24 °C) by iodine catalysis (2% $I_2$) in diffuse daylight (○——○ all-*trans*, ●——● 9-*cis*, □——□ 13(15)-*cis*, ▲—▲ mixture of di-*cis*-isomers)

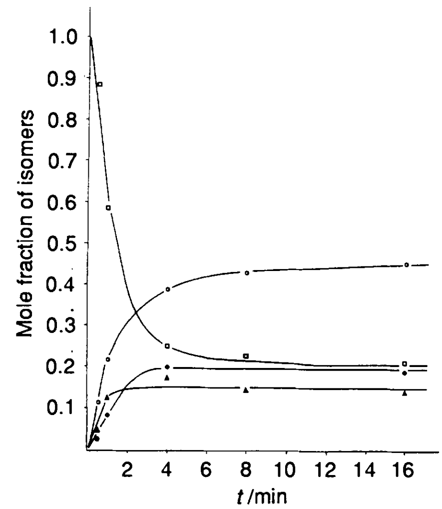

**Fig. 4** Isomerization of 13(15)-*cis*-zeaxanthin [13(15)-*cis*-**2**] ($10^{-4}$ mol dm$^{-3}$ in benzene, 24 °C) by iodine catalysis (2% $I_2$) in diffuse daylight (○——○ all-*trans*, ●——● 9-*cis*, □——□ 13(15)-*cis*, ▲——▲ mixture of di-*cis*-isomers)

*Specific Rate Experiments*.—Earlier it had been assumed that, in the process of iodine-catalysed photoisomerization of carotenoids, a free radical[5,20,27] was formed on the addition of iodine. Weak chemical interactions[28–31] were also proposed for this 'adding and breaking' mechanism. During the last 20 years, the Raman and absorption spectra of β-carotene (**1**)–iodine mixtures[32,33] (in various solvents) and Mössbauer[34] and EPR measurements[35] have revealed that β-carotene forms cation radicals[35] at 300 K according to $2C_{40}H_{56} + 3I_2 \rightleftharpoons 2C_{40}H_{56}{}^{\cdot+} + 2I_3{}^-$. Probably the traces of cation radical present in the isomerization mixtures are responsible for the very slow *cis–trans* stereomutation in darkness (Fig. 1). It was assumed that, in the presence of light, the equilibrium between a carotenoid and iodine was shifted towards the formation of carotenoid cation radicals. Thus the rate of photoisomerization of a carotenoid was increased through the formation of more carotenoid cation radicals, which took part in the *cis–trans* isomerization process, either as intermediates[31,33,34] or photocatalysts.[35]

---

* 13(15)-*cis* = 13-*cis* + 15-*cis* (mixture of 13- and 15-*cis*-isomers).

**Table 2** Functions of the disappearance or formation of geometrical isomers of zeaxanthin (**2**) until quasi-equilibrium is reached (correlation indexes and coefficients[26] are in parentheses)

| | Products of *cis–trans* isomerization | | | |
|---|---|---|---|---|
| Starting material | all-*trans* | 9-*cis* | 13(15)-*cis* | di-*cis* |
| all-*trans* | $Y_1{}^*(0.793)$ | $Y\begin{pmatrix}0.992\\-0.597\end{pmatrix}$ | $Y_2{}^*(0.906)$ | $Y_2{}^*(0.884)$ |
| 9-*cis* | $Y\begin{pmatrix}0.931\\-0.919\end{pmatrix}$ | $Y\begin{pmatrix}-0.936\\-0.933\end{pmatrix}$ | $Y_2{}^*(0.818)$ | $Y\begin{pmatrix}0.864\\0.894\end{pmatrix}$ |
| 13(15)-*cis* | $Y_2{}^*(0.938)$ | $Y_2{}^*(0.889)$ | $Y\begin{pmatrix}-0.998\\-0.925\end{pmatrix}$ | $Y\begin{pmatrix}0.981\\-0.588\end{pmatrix}$ |

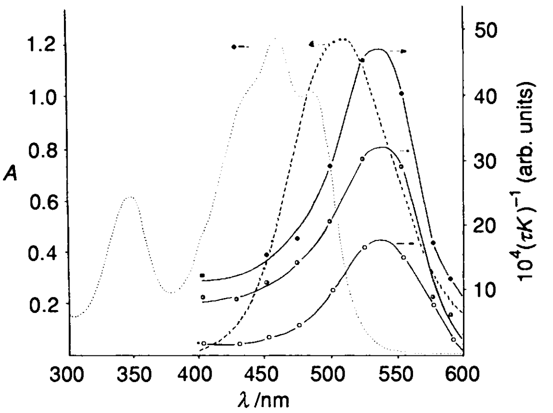

Fig. 5 'Specific rate' $[(\tau K)^{-1}]$ of isomerization of 13-*cis*-zeaxanthin (13-*cis*-**2**) ($2 \times 10^{-5}$ mol dm$^{-3}$ in benzene, 24 °C) *vs.* wavelength of irradiation (mole ratio of 13-*cis*-zeaxanthin and $I_2$ = 26.6 ○——○; 13.3 ◑——◑; 6.65 ●——●); UV–VIS spectrum of 13-*cis*-zeaxanthin (· · · ·) and iodine (– – – –) in benzene

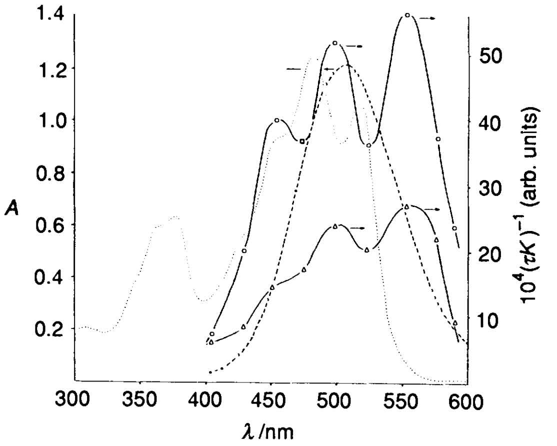

Fig. 6 'Specific rate' $[(\tau K)^{-1}]$ of isomerization of 13-*cis*-capsorubin (13-*cis*-**6**) ($2 \times 10^{-5}$ mol dm$^{-3}$ in benzene, 24 °C) *vs.* wavelength of irradiation (mole ratio of 13-*cis*-capsorubin and $I_2$ = 26.6 ○——○; 13.3 ▲——▲); UV–VIS spectrum of 13-*cis*-capsorubin (· · · ·) and iodine (– – – –) in benzene

Experiments designed to measure the specific rates of *cis–trans* isomerization (adjusted to the intensity of irradiation) of different carotenoids may open up new areas of investigation into the mechanism of (*Z*/*E*)-photoisomerization of carotenoids in the presence of iodine.

Dependence of the rate of *cis–trans* isomerization upon the wavelength of incident light in the visible region was investigated by using a set of metal interference filters. In Figs. 5–7, the specific rates of *cis–trans* isomerization $[10^4(\tau K)^{-1}]$ of different 13-*cis* carotenoids (see Table 3) are plotted against the wavelength of irradiation. For comparison the UV–VIS spectra of the 13-*cis* carotenoids and iodine, in arbitrary concentrations, in benzene solution, are also plotted.

The plots fall into two types: curves (Fig. 5) with one maximum (13-*cis*-**2**) and curves (Figs. 6, 7) with more than one maximum (13-*cis*-**6** and 13-*cis*-**7**).

The different characters of the curves are due to the presence or absence of a carbonyl group in the chromophoric system. Conjugation of the polyene chain with a carbonyl group, rather than the other end groups, determines the character of the plots. For example, 13-*cis*-capsanthol (**9**) (obtained from 13-*cis*-**7** by $NaBH_4$) without a carbonyl group has a Gaussian-type curve (Fig. 7). Although the experimental data cannot be explained yet, the following comments can be made.

(*a*) In the curves (Figs. 5–7), the maxima have different locations: the shift between the position of the specific rate maximum at the longest wavelength and that of the absorption maximum at the longest wavelength varies from 36 to 49 nm [$\Delta\lambda$(13-*cis*-**2**) = 536 − 487 = 49 nm, $\Delta\lambda$(13-*cis*-**6**) = 553 − 517 = 36 nm, $\Delta\lambda$(13-*cis*-**9**) = 523 − 478 = 45 nm]. Similarly, there is no definite $\Delta\lambda$ shift between the position of the specific rate maximum at the longest wavelength and that of the absorption maximum of iodine [$\Delta\lambda$(13-*cis*-**2**) = 30 nm, $\Delta\lambda$(13-*cis*-**6**) = 46 nm, $\Delta\lambda$(13-*cis*-**7**) = 46 nm and $\Delta\lambda$(13-*cis*-**9**) = 17 nm].

(*b*) Since both *trans* and *cis* carotenoids in solution react with electrophiles (Carr–Price reaction, $I_2$, HCl, *etc.*) to yield strongly-coloured charge-transfer complexes,[31,33,34] which might be involved in the *cis–trans* isomerization process, the position of the specific rate maximum of **7** (Fig. 7) at the longest wavelength maximum is related to that of the absorption maximum of the charge transfer complex. It can only be stated that the position of the specific rate maximum at the longest wavelength is located in the region between the absorption maximum at the longest wavelength and that of a corresponding charge-transfer complex.

## Experimental

*General.*—UV–VIS spectra were recorded on a Perkin-Elmer 402 spectrophotometer. *Q* values indicate $A_{max}/A_{cis\text{–}peak}$; ε values are given in dm$^3$ mol$^{-1}$ cm$^{-1}$ in parentheses. The general methods of handling carotenoids and column chromatography have been described elsewhere.[12]

*Materials.*—Either analytical carotenoids were taken directly from our own collection, or the unstable *cis* isomers were freshly prepared from the corresponding *trans* isomers. β-Carotene (**1**): $\lambda_{max}(C_6H_6)$/nm 494 (106 100), 464 (122 300); 9-*cis*-**1** $\lambda_{max}(C_6H_6)$/nm 489, 460; 13(**15**)-*cis*-**1** $\lambda_{max}(C_6H_6)$/nm 486, 456 and 348, *Q* = 2.76. Zeaxanthin (**2**): $\lambda_{max}(C_6H_6)$/nm 493 (107 300), 463 (124 200); 9-*cis*-**2**[7,11] $\lambda_{max}(C_6H_6)$/nm 488 (94 700), 458

**Table 3** Time constants (τ) and 'specific rate' values [$10^4$ $(\tau K)^{-1}$, in arb. units] obtained by isomerization of several 13-*cis*-carotenoids using different types of metal interference filters

| Data of filters (VEB Carl Zeiss JENA) | | | | 13-*cis*-carotenoids | | | | | | | |
|---|---|---|---|---|---|---|---|---|---|---|---|
| | | | | 13-*cis* **2** | | 13-*cis*-**6** | | 13-*cis*-7 | | 13-*cis*-**9** | |
| Type | $\lambda_{max}$/nm | *T*(%) | $\Delta\lambda$/nm | τ/min | $10^4(\tau K)^{-1}$ | τ/min | $10^4(\tau K)^{-1}$ | τ/min | $10^4(\tau K)^{-1}$ | τ/min | $10^4(\tau K)^{-1}$ |
| Na 590 J | 593.8 | 21.66 | 14.0 | 104.0 | 2.40 | 10.5 | 23.81 | 25 | 10.00 | 32 | 7.81 |
| IF-575 | 576.0 | 34.17 | 8.5 | 38.0 | 7.53 | 7.3 | 39.22 | 20 | 14.32 | 21 | 13.63 |
| IF-550 | 551.9 | 40.05 | 8.0 | 20.5 | 15.05 | 5.3 | 58.22 | 13 | 23.73 | 11 | 28.05 |
| IF-525 | 521.9 | 41.10 | 7.5 | 24.8 | 16.47 | 11.3 | 36.15 | 22 | 18.57 | 13 | 31.43 |
| IF-500 | 498.0 | 37.53 | 5.5 | 78.0 | 9.82 | 14.8 | 51.73 | 34 | 22.52 | 26 | 29.45 |
| IF-475 | 473.5 | 43.13 | 7.0 | 154.5 | 4.42 | 18.5 | 36.91 | 47 | 14.53 | 55 | 12.42 |
| IF-450 | 454.5 | 27.48 | 6.0 | 580 | 2.72 | 39.5 | 39.88 | 140 | 11.25 | 280 | 5.63 |
| IF-425 | 428.8 | 39.38 | 7.5 | 750 | 1.70 | 63.8 | 19.95 | 200 | 6.37 | 270 | 4.71 |
| UV-IF-400 | 403.2 | 37.41 | 8.0 | 1140 | 1.72 | 270.0 | 7.28 | 445 | 4.42 | 365 | 5.39 |

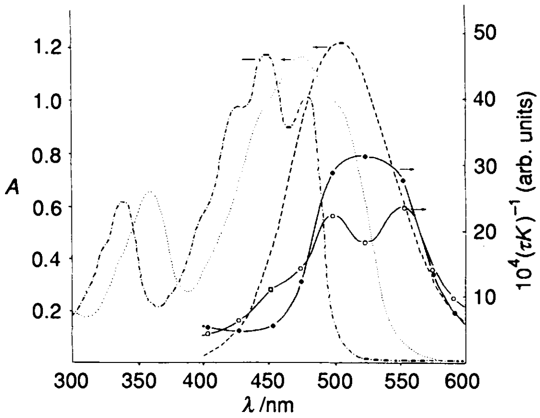

**Fig. 7** 'Specific rate' [$(\tau K)^{-1}$] of isomerization of 13-*cis*-capsanthin (13-*cis*-7) (○——○) and 13-*cis*-capsanthol (13-*cis*-9) (●——●) ($2 \times 10^{-5}$ mol $dm^{-3}$ in benzene, 24 °C, mole ratio of carotenoid and $I_2$ = 26.6) *vs.* wavelength of irradiation; UV–VIS spectra of 13-*cis*-capsanthin (· · ·), 13-*cis*-capsanthol (— · — · —) and iodine (– – – –) in benzene

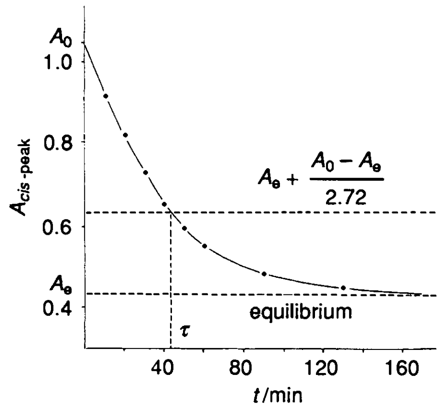

**Fig. 8** Determination of time constants (τ-values) measured by the change of intensity of the *cis*-peak with time

(10 700) and 348 (8800); 13(15)-*cis*-**2**[7–11] $\lambda_{max}(C_6H_6)$/nm 487 (70 200), 458 (86 300) and 347 (39 000), *Q* = 2.12; 15-*cis*-**2** $\lambda_{max}(C_6H_6)$/nm 487, 459 and 347, *Q* = 1.60. Physaliene (**3**): $\lambda_{max}(C_6H_6)$/nm 493 and 463. 3*S*,5*R*,6*S*,3′*S*,5′*R*,6′*S*-Violaxanthin (**4**): $\lambda_{max}(C_6H_6)$/nm 483 (130 900), 453 (135 400) and 426 (88 900); 9-*cis*-**4**[10,12,13] $\lambda_{max}(C_6H_6)$nm 478 (121 000), 448 (125 400) and 424 (82 300); 13-*cis*-**4**[10,13] $\lambda_{max}(C_6H_6)$/nm 475 (99 700), 445 (115 200), 419 (81 200) and 337 (59 000), *Q* = 2.00; 15-*cis*-**4**[10,13,15] $\lambda_{max}(C_6H_6)$/nm 478 (81 000), 448 (95 000), 423 (68 000) and 337 (58 000), *Q* = 1.61. 3*S*,5*S*,6*R*,3′*S*,5′*S*,6′*R*-Violaxanthin (**5**) $\lambda_{max}(C_6H_6)$/nm 483 (130 900), 453 (135 400) and 426 (8900); 9-*cis*-**5** $\lambda_{max}(C_6H_6)$/nm 478 (121 000), 448 (125 400) and 424 (82 300); 13(15)-*cis*-**5** $\lambda_{max}(C_6H_6)$/nm 476 (96 900), 446 (112 200), 420 (74 200) and 337 (59 000), *Q* = 1.95. Capsorubin (**6**) $\lambda_{max}(C_6H_6)$/nm 522 (119 100), 487 (129 800) and 463 (89 200); 9-*cis*-**6**[7,11] $\lambda_{max}(C_6H_6)$/nm 519 (99 000), 485 (111 000) and 380 (16 000); 13-*cis*-**6**[7,11] $\lambda_{max}(C_6H_6)$/nm 517 (71 000), 483 (86 000) and 378 (40 000), *Q* = 2.15. Capsanthin (**7**) $\lambda_{max}(C_6H_6)$/nm 486 (113 200); 9-*cis*-**7**[14] $\lambda_{max}(C_6H_6)$/nm 482 (90 000); 13-*cis*-**7**[14] $\lambda_{max}(C_6H_6)$/nm 478 (79 200) and 361 (44 400), *Q* = 1.78; 9′-*cis*-**7**[14] $\lambda_{max}(C_6H_6)$/nm 478 (93 000); 13′-*cis*-**7**[14] $\lambda_{max}(C_6H_6)$/nm 476 (78 100) and 360 (44 000), *Q* = 1.78. 3*S*,5*R*,6*S*,3′*R*,6′*R*-Lutein-epoxide (**8**) $\lambda_{max}(C_6H_6)$/nm 483 (120 400), 452 (125 100) and 427 (84 600); 9-*cis*-**8**[7,18] $\lambda_{max}(C_6H_6)$/nm 478 (105 600), 448 (115 000) and 423 (86 400); 9′-*cis*-**8**[7,18] $\lambda_{max}(C_6H_6)$/nm 478 (96 500), 449 (101 200) and 424 (77 900); 13-*cis*-**8**[7,18] $\lambda_{max}(C_6H_6)$/nm 475 (58 600), 445 (68 000), 420 (45 400) and 337 (34 800), *Q* = 1.95; 13′-*cis*-**8**[7,18] $\lambda_{max}(C_6H_6)$/nm 476 (71 100), 446 (82 800), 420 (60 300) and 337 (43 900), *Q* = 1.88; 15-*cis*-**8**[18] $\lambda_{max}(C_6H_6)$/nm 478, 448, 424 and 337, *Q* = 1.70. Capsanthol (**9**) $\lambda_{max}(C_6H_6)$/nm 487 (120 300), 457 (128 200) and 434 (94 400); 13-*cis*-**9** $\lambda_{max}(C_6H_6)$/nm 478, 449 and 339, *Q* = 2.03.

*Equilibrium Measurements.*—For comparison of the equilibrium concentrations with the data in the literature, the experiments were carried out in scattered daylight in $10^{-4}$ mol $dm^{-3}$ benzene solutions (100 $cm^3$) in the presence of 2% iodine relative to the amount of carotenoid, at 24–25 °C under nitrogen. The isomerizations were monitored by UV spectrophotometry; and, when equilibrium was reached, the benzene solutions were washed free of iodine in a separating funnel with 5% $Na_2S_2O_3$. After the usual work-up, the equilibrium mixtures were separated on a calcium carbonate column ('Biogal', Hungary) with a 1:1 mixture of benzene and hexane (zeaxanthin), with benzene (violaxanthins), with benzene containing acetone gradually increased up to 0.3% (lutein epoxide), 1% (capsanthin) or 2% (capsorubin).

*Rate Measurements.*—Kinetic experiments were performed in $2 \times 10^{-5}$ mol $dm^{-3}$ benzene solutions of 13-*cis* carotenoids at 24–25 °C under nitrogen. Aliquot stock solutions of a 13-*cis* carotenoid and iodine were mixed in a quartz cell of 10 mm diameter and 3 $cm^3$ volume in the dark: the mole ratio of carotenoid to iodine was 26.6. The freshly prepared solution was irradiated with a Tungsram Krypton Superba opal lamp (60 W) equipped with a set of metal interference filters (VEB Carl Zeiss

JENA, see Table 3) from a distance of 16 cm. External air blasts were concentrated on the lamp to keep the temperature constant. Because, in contrast to all-*trans* (and 9-*cis*) carotenoids, 13-*cis* (and 15-*cis*) isomers exhibit a high *cis*-peak in the ultraviolet region, the changing ratio of the isomeric forms can be measured over time by spectroscopy. The irradiation was continued until the original $A_{cis}$-value ($A_0$) fell to that of $A_{\text{equilibrium}} + [(A_0 - A_{\text{equilibrium}})/2.72]$ (Fig. 8).

## Acknowledgements

We thank Mrs. M. Steiler for skilful assistance and L. Koszorus for computations of the experimental data.

## References

1 P. Karrer, A. Helfenstein, R. Widmer and Th. B. van Itallie, *Helv. Chim. Acta*, 1929, **12**, 741.
2 L. Zechmeister and P. Tuzson, *Ber. Dtsch. Chem. Ges.*, 1939, **72**, 1340.
3 L. Zechmeister, L. Cholnoky and A. Polgár, *Ber. Dtsch. Chem. Ges.*, 1939, **72**, 1678.
4 L. Zechmeister and R. M. Lemmon, *J. Am. Chem. Soc.*, 1944, **66**, 317.
5 L. Zechmeister, *Cis–Trans Isomeric Carotenoids, Vitamins A and Arylpolyenes*, Springer, Wien, 1962.
6 O. Isler, *Carotenoids*, Birhäuser, Basle, 1971.
7 J. Szabolcs, *Pure Appl. Chem.*, 1976, **47**, 147.
8 L. Liaaen-Jensen, *Fortschr. Chem. Org. Naturst.*, 1980, **39**, 123.
9 T. W. Goodwin, *Carotenoid Chemistry and Biochemistry*, eds. G. Britton and T. W. Goodwin, Pergamon Press, Oxford, 1981.
10 J. Szabolcs, *Plant Carotenoids*, in *Carotenoinds, Chemistry and Biology*, eds. N. I. Krinsky, M. M. Mathews-Roth and R. F. Taylor, Plenum Press, New York, 1989, p. 39.
11 M. Baranyai, J. Szabolcs, Gy. Tóth and L. Radics, *Tetrahedron*, 1976, **32**, 867.
12 P. Molnár and J. Szabolcs, *Acta Chim. Acad. Sci. Hung.*, 1979, **99**, 155.
13 P. Molnár and J. Szabolcs, *Phytochemistry*, 1980, **19**, 623.
14 M. Baranyai, P. Molnár, J. Szabolcs, L. Radics and M. Kajtár-Peredy, *Tetrahedron*, 1981, **37**, 203.
15 L. Radics, P. Molnár and J. Szabolcs, *Phytochemistry*, 1983, **22**, 306.
16 P. Molnár, L. Radics and J. Szabolcs, *Acta Chim. Acad. Sci. Hung.*, 1983, **112**, 477.
17 P. Molnár, J. Szabolcs and L. Radics, *Phytochemistry*, 1986, **25**, 195.
18 J. Deli, P. Molnár, J. Szabolcs, Gy. Tóth and L. Radics, *Phytochemistry*, 1988, **27**, 547.
19 R. S. H. Liu and A. E. Asato, *Tetrahedron*, 1984, **40**, 1931.
20 P. Zscheile, R. H. Harper and H. A. Nash, *Arch. Biochemistry*, 1944, **5**, 211.
21 C. A. Pesek and J. J. Warthesen, *J. Agric. Food Chem.*, 1990, **38**, 1313.
22 K. Jorgensen and L. H. Skibsted, *Z. Lebensm. Unters. Forsch.*, 1990, **190**, 306.
23 M. Kuki, Y. Koyama and H. Nagae, *J. Phys. Chem.*, 1991, **95**, 7171.
24 A. A. Frost and R. G. Pearson, *Kinetics and Mechanism*, J. Wiley, New York, 1953.
25 Z. G. Szabó, in *Comprehensive Chemical Kinetics*, ed. C. H. Bamford, C. F. H. Tipper, Elsevier Publishing Company, Amsterdam, London, New York, 1969, vol. 2, ch. 1.
26 N. R. Draper and H. Smith, *Applied Regression Analysis*, 2nd edn., John Wiley, New York, 1981.
27 M. S. Kharasch, J. V. Mansfield and F. R. Mayo, *J. Am. Chem. Soc.*, 1937, 59, 1155.
28 R. Willstätter and W. Mieg, *Liebigs. Ann. Chem.*, 1907, **355**, 1.
29 L. Zechmeister and L. v. Cholnoky, *Liebigs. Ann. Chem.*, 1930, **478**, 103.
30 P. Karrer and O. Walker, *Helv. Chim. Acta*, 1934, **17**, 43.
31 J. H. Lupinsky, *J. Phys. Chem.*, 1963, **67**, 275.
32 I. Harada, Y. Furukawa, M. Tasumi, H. Shirakawa and S. Ikeda, *Chem. Lett.*, 1980, **3**, 267.
33 A. Slama-Schwok, M. Blanchard-Desce and J.-M. Lehn, *J. Phys. Chem.*, 1990, **94**, 3894.
34 T. Matsuyama, H. Sakai, H. Yamaoka and Y. Maeda, *J. Chem. Soc., Dalton Trans.*, 1982, 229.
35 R. Ding, J. L. Grant, R. M. Metzger and L. D. Kispert, *J. Phys. Chem.*, 1988, **92**, 4600.

*Paper* 2/02404G
*Received* 11*th May* 1992
*Accepted* 2*nd October* 1992